Annals of Biomedical Engineering, Vol. 20, pp. 41–62, 1992
Printed in the USA.

0090-6964/92 $5.00 + .00

Ventriculo-Arterial Coupling: Concepts, Assumptions, and Applications

David A. Kass and Raymond P. Kelly

Division of Cardiology
Johns Hopkins Medical Center
Baltimore, MD

(Received 4/25/91)

Recent investigations have yielded new insights into the interaction of the left ventricle with the arterial system. These studies have employed a variety of coupling frameworks to quantify this interaction, and each makes several simplifying assumptions. In this article, we review these frameworks, their major findings, assumptions, and clinical applications, and examine future directions for this research.

Keywords—*Ventricular function, Ventricular pressure-volume relations, Arterial impedance, Stroke work, Ventricular efficiency, Vascular load, Matching.*

INTRODUCTION

Eight years ago, in this journal, a series of review articles presented theoretical models and experimental results from studies of ventriculo-arterial interaction (42,52,57). These papers posed a number of key questions: (a) Could coupling frameworks be designed that characterized both ventricular and vascular properties, and provide accurate predictions of integrated function variables such as stroke volume, stroke work, or mean arterial pressure and flow? (b) If so, then how did the ventricle couple to the arterial system *in vivo* under varying conditions? Specifically, did coupling occur such that ventricular power (or stroke work) or energetic efficiency was optimized? (c) What determined or controlled the equilibrium working point of ventriculo-arterial coupling in intact systems? (d) How was coupling altered by acute pharmacologic interventions or disease conditions?

Since the appearance of these reviews, numerous studies have examined these and other issues relevant to ventriculo-vascular coupling. With new insight has come an increasing appreciation for the complexity of both ventricular and arterial properties and their characterizations, raising concerns over the applicability of the simplified models generally employed. Recent data in intact animals and human subjects are testing many of these coupling concepts and hypotheses within more meaningful and clinically relevant physiologic settings; both normal and diseased. In this review, we will

Acknowledgments—This work was supported by the National Institutes of Health Physician Scientist Award HL-01820 (DAK); The National Heart Foundation of Australia Overseas Fellowship, Fulbright Scholarship; and The Royal Australasian College of Physicans Travelling Grant (RPK).

Address correspondence to David A. Kass, M.D., Carnegie 565B, Johns Hopkins Hospital, 600 N. Wolfe Street, Baltimore, MD 21205.

critically examine the major coupling frameworks and their assumptions, and report on studies that have sought to answer the questions posed above.

COUPLING MODELS

> "Although this may seem a paradox, all exact science is dominated by the idea of approximation."
>
> Bertrand Russell

From the outset, linking the ventricle with the vasculature presents a language problem. Due to the anatomic complexities of the vascular tree and the pulsatile nature of aortic flow, it is generally agreed that characterization of the vascular load is most complete in the frequency domain in the form of impedance spectra (33,41). Furthermore, to provide as much frequency content as possible, the spectra should ideally be derived from pressure and flow data driven by white noise, i.e., random cardiac cycle lengths (5,54). While it may arguably be more difficult to agree on a "best" way to characterize ventricular properties, a description in the frequency domain from data obtained during random pacing would not be among those considered.

To describe and predict the behavior of the coupled system, investigators have therefore simplified the problem primarily by de-emphasizing the pulsatile nature of pressure/flow, and thus reducing the impedance spectra information to a mean total resistance (R_p). In the framework of Van den Horn, Elzinga, and Westerhof (56–58), this resistance is coupled to a ventricular "source resistance" (R_s determined from a mean ventricular pressure-flow function curve). Coupling requires a constant relation between mean arterial (mABP) and mean ventricular (mLVP) pressure, which was first reported for the open chest cat (58), thereby enabling the vascular line (mean pressure vs. flow) to be plotted on the same ventricular pump function graph. The intersection of ventricular and vascular relations determines the system working point (Fig. 1a). This approach has the advantage of utilizing readily measurable function parameters (pressures and flows) and has yielded many insights regarding coupling and power optimization. However, there are disadvantages. The mean pressure-flow relation is influenced by preload volume (10,31) and changes in characteristic impedance (31) and it is nonlinear, making the "source" resistance, itself a function of flow. It is also less able to incorporate aspects of diastolic function and energetics into the overall coupling schema.

An alternative approach based on pressure-volume relations was proposed by Sunagawa *et al.* (50,51,53). Vascular impedance is distilled into an effective arterial elastance (Ea) (31), which can be easily coupled with ventricular pressure-volume loops and relations. The approach approximates mean and end-ejection arterial pressure by the ventricular end-systolic pressure. Employing a 3-element Windkessel vascular model, it predicts that the ratio of end-systolic pressure (P_{es}) to stroke volume (SV) is constant under a given steady state vascular impedance load, and is given by:

$$P_{es}/SV \approx R_T/[t_s + \tau(1 - e^{-t_d/\tau})] = Ea \tag{1}$$

with t_s, t_d, and τ the systolic and diastolic time periods and diastolic pressure decay time constant ($=RC$ product of the 3-element Windkessel electrical analogue), respectively. Under normal operating conditions, the predominant factors influencing Ea are total series resistance (R_T) and heart rate ($Ea \approx R_T \cdot HR$). Drawn as a line with

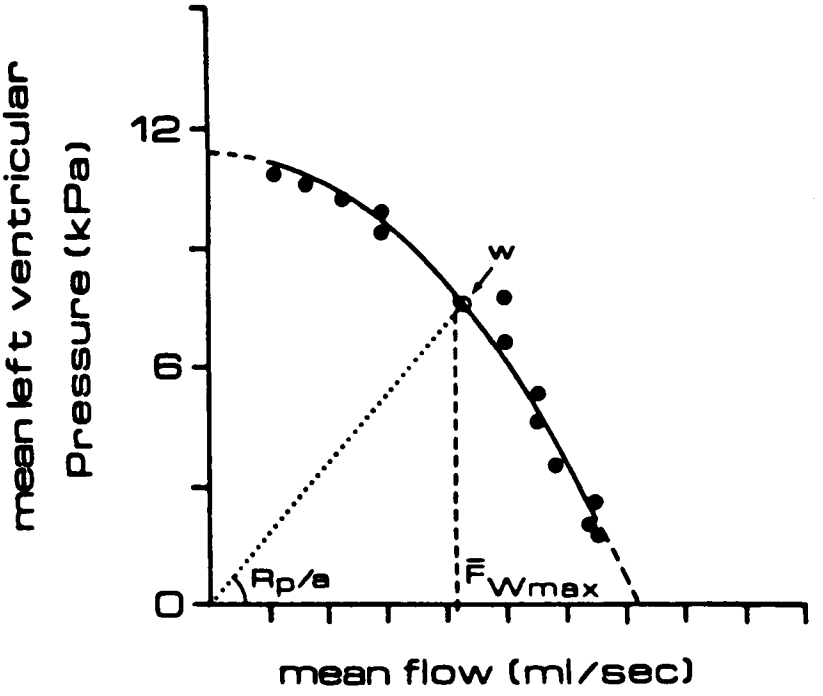

FIGURE 1. (a) ***Pressure-flow coupling framework.*** **Mean ventricular pressure-flow relation at a given end-diastolic volume, heart rate, and contractility. Arterial load is varied and the resulting mean LV pressure and flow which are inversely related are obtained. The working point of the heart (W) is the intersection of the arterial resistance line (with a conversion factor *a* relating mean ventricular to mean arterial pressure) with the pump function curve (56). (Reprinted by permission of The American Physiological Society.)**

slope ($-Ea$) starting at the point (EDV,0), this vascular relation intersects the end-systolic pressure-volume relation at a given P_{es}, which is the ventriculo-arterial coupling point (Fig. 1b). A hybrid approach, proposed by Myhre and Piene *et al.* (36), relates pressure-volume data to mean arterial resistance in an analagous manner.

While the specifics differ, there are several underlying assumptions common to these approaches. Each assumes that the model parameters are state variables, i.e., descriptions of ventricular and vascular properties that are essentially independent of each other. Thus, in the pressure-volume framework, the end-systolic elastance (*Ees*), the slope of the end-systolic pressure-volume relation, is assumed to be relatively linear and independent of altered vascular loading (volumes or impedance changes); such that changes in this parameter primarily reflect ventricular contractile performance. A similar statement holds for the source resistance derived from ventricular mean pressure-flow function curves. Vascular properties are also assumed to be "linear" so that mean resistance (or arterial elastance) is independent of operating pressures or flows. Pulsatile behavior is ignored in models using mean resistance as the coupling variable, whereas the effective arterial elastance is influenced to a small but definite degree by vascular compliance and characteristic impedance changes (51) (see Eq. 1). Rather than being a disadvantage (36), this may be helpful when coupling is studied in aging or hypertensive subjects with frequently prominent pulsatile components.

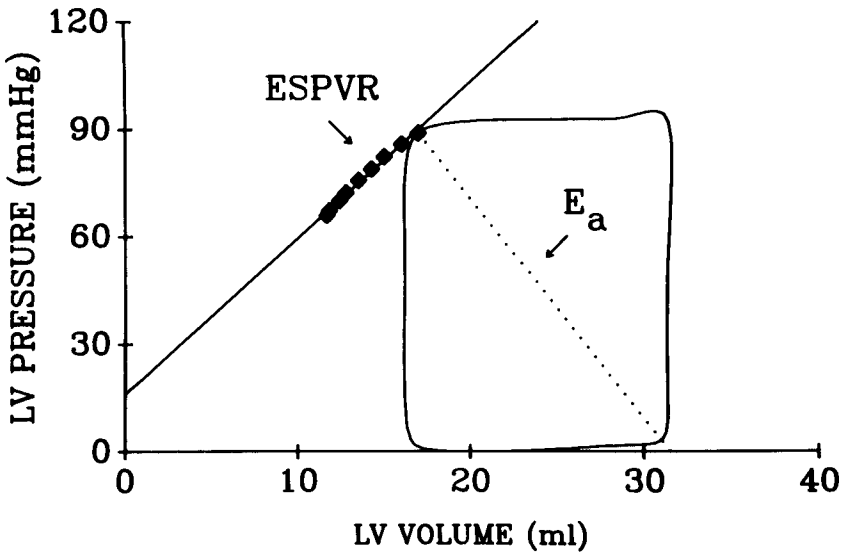

FIGURE 1. (b) *Pressure-volume coupling framework.* Ventricular systolic function is assessed by the end-systolic pressure-volume relation (solid symbols) obtained from pressure-volume loops at varying loads. The steady state effective vascular elastance (*Ea*) is equal to the ratio of end-systolic pressure (P_{es}) to stroke volume, and is shown by the diagonal dotted line. The intersection of both points at a common P_{es} is the equilibrium point.

While most ventriculo-vascular coupling studies have used simplified impedance models, it should be noted that a few investigators have attempted to link frequency domain descriptions of the vasculature with pressure-volume descriptions of ventricular function (5,26,43). Until recently, this was performed using data obtained at steady state heart rates (26,43), however the resulting limited frequency information has prevented straightforward calculation of the impulse response function (IRF), used to predict pressure and flow waveforms in the time domain. In a recent part-experimental, part-modeling study, Burkhoff *et al.* (5) obtained high resolution impedance spectra during random pacing and used this to derive an impulse response function (relating arterial pressure response to a single flow "pulse"). By this approach, the vascular load could be imposed by convolution on a model heart (time-varying elastance) to predict pump function. We discuss the results of this study later, but it is important to note that this coupling analysis was based on predicted responses of a model heart. How real impedance loads impact on real beating hearts, particularly loads with abnormal reflections and hearts with myocardial disease, remains unknown.

TESTING THE ASSUMPTIONS

"Seek simplicity and distrust it."

Whitehead

I. Ventricular Properties

Load Interactions. Assessment of cardiac systolic performance by the end-systolic pressure-volume relationship (ESPVR) obtained from multiple pressure-volume loops

under varying loads has been extensively and successfully employed in isolated (45) and intact animal studies (21,47) as well as in humans (20,32). In models of ventriculovascular coupling, this relation is often used to represent the contractile performance of the heart. Thus, a key question is whether the ESPVR itself is influenced by changes in chamber volumes or vascular impedance loading. In isolated blood perfused canine hearts contracting against a simulated arterial load (3-element Windkessel), Maughan *et al.* (30) found that four fold variations in arterial compliance or characteristic impedance had little effect on the ESPVR. Changes in arterial resistance, however, led to a small but consistent left or rightward shifts (with increased or decreased resistance, respectively) of the entire end-systolic pressure relation. Similar shifts were subsequently reported by Freeman *et al.* (12) *in vivo.* This effect was ascribed to a negative influence of ejection on systolic performance due to an internal ventricular resistance (29,46), i.e.,

$$P(t) = E(t)(V(t) - V_o) - R \cdot dV(t)/dt \ . \tag{2}$$

Greater ejection and thus higher flow rates would lower the end-systolic ventricular pressure below the level achieved with less or no ejection, resulting in a rightward ESPVR shift.

More recently, however, several studies have reported opposing positive effects of ejection on the end-systolic pressure and pressure-volume relation. In one study, Hunter (13) compared the end-systolic pressure of ejecting beats to the first beat after a sudden switch to isovolumic contraction mode, maintaining the end-systolic volume the same for both beats. An internal resistance would always lower P_{es} for ejecting beats; yet, the data frequently revealed the opposite. The extent of positive ejection influence depended on the amount of the ejection and the end-diastolic volume (EDV) of the ejecting beat. For beats with ejection fractions greater than 50–60% (starting at larger end-diastolic volumes), P_{es} exceeded that of the isovolumic beat at the identical end-systolic volume (V_{es}), whereas those with small ejection fractions (and smaller EDVs) had a lower P_{es} than isovolumic contraction. Among the explanations for the positive ejection effect was that ejecting beats started at a higher EDVs (fiber lengths), and enhanced length dependence of calcium activation resulted in greater contractile performance.

We have recently extended these observations to the entire ESPVR (6). Steady state beats at four randomly chosen preload volumes were obtained under isovolumic and ejecting conditions, with arterial resistance varied for the ejecting beats. Our results also revealed a positive effect of ejection particularly for beats with physiologic ejection fractions (Fig. 2, upper panel). In addition to mechanical effects, we also found ejection had an interesting favorable effect on myocardial energetics (Fig. 2, lower panel). Specifically, using the relation described by Suga *et al.* (48) between oxygen consumption and pressure-volume area to assess myocardial efficiency, we found small but significant improvement in efficiency for ejecting versus isovolumic contractions, which was also magnified at physiologic EFs. Thus, in addition to having potentially complex influences on the ESPVR, ejection also appears to alter energetics making prediction of efficiency and work optimization from coupling relations a more complex problem.

At the present time, it is difficult to know whether these effects observed under extreme conditions in isolated heart preparations pertain to normal (or abnormal) intact physiologic conditions. In an attempt to examine ejection history effects on

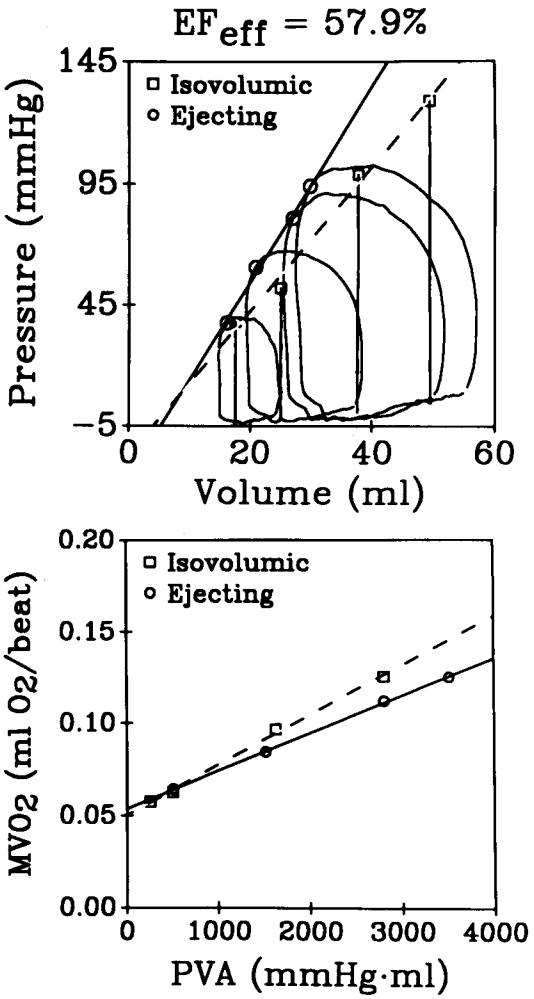

FIGURE 2. Effect of physiologic afterload on end-systolic pressure-volume relation (top panel) and myocardial oxygen consumption–pressure-volume area relation (bottom panel) in isolated canine heart. Switching from isovolumic contraction (dashed relations) to ejection at an effective ejection fraction of 58% ($EF_{eff} = SV/(V_{ed} - V_o)$), produced an increase in the slope of the ESPVR and a downward displacement of the MVO_2-PVA relation. Thus, ejection favorably influenced both contractile performance and efficiency.

ESPVRs in human subjects, we determined pressure-volume relations during transient preload reduction (balloon occlusion of the inferior vena cava, IVC) versus afterload increase (sudden maximal isometric handgrip). In 7 out of 13 patients there was virtually no difference in ESPVRs, and we have previously presented a typical example of this response (18). For the overall group, mean ESPVR slope by IVC occlusion was 2.3 mmHg/ml versus 3.3 mmHg/ml by handgrip. However, handgrip also led to a significant increase in heart rate from 82 ± 15 to 91 ± 16 min^{-1} ($p < .05$) (IVC occlusion did not), and thus reflex effects likely complicated the comparison.

There is also little or no data regarding the impact of abnormal vascular loads such as accompany aging or arteriosclerosis on ventricular mechanics and efficiency. Such vascular changes can pose additional loads on the heart due to late systolic wave reflections and reduced vascular compliance, and could also influence ventricular performance. One isolated heart study performed using a single tube model for the impedance load found little influence of wave reflections on the ESPVR (14), however, whether more realistic abnormal loads affect ventricular function remains to be studied. Further work is clearly needed.

ESPVR Curvilinearity. Another complicating factor regarding use of the ESPVR and particularly its slope (*Ees*) in ventriculo-vascular coupling analysis is nonlinearity of the relation. Contractility dependent ESPVR nonlinearity has been reported in the isolated (8) and *in vivo* heart (16). Certainly, substantial nonlinearity poses a problem for coupling analyses, since the pump function variable Ees itself becomes a function of operating pressure and thus vascular loading conditions. This problem, however, is no different from that posed by the parabolic mean ventricular pressure-flow relation (10,57), which also leads to load-dependent estimation of the ventricular source resistance.

While a linear systolic function relation is certainly convenient, it is not essential to coupling analysis, and equations for nonlinear ESPVRs analogous to those derived for the linear case can be obtained. For example, in the linear ESPVR model, the ventricle is represented by:

$$P_{es} = Ees(V_{es} - V_o) = Ees(V_{ed} - V_o - SV) \tag{3}$$

and the arterial system by:

$$P_{es} = Ea \cdot SV \ . \tag{4}$$

The coupled system operates at a given P_{es}, thus the two equations are equated and solved for stroke volume:

$$SV = \frac{Ees(V_{ed} - V_o)}{Ees + Ea} \tag{5}$$

or stroke work (approximated by the product of SV and end-systolic pressure):

$$SW = P_{es} \cdot SV = Ea \cdot SV^2 = Ea[Ees(V_{ed} - V_o)/(Ees + Ea)]^2 \ . \tag{6}$$

Using this last expression, for a given *Ees*, one can predict that maximal SW will occur when $Ees = Ea$ (differentiating Eq. 6 with respect to *Ea*, setting the result = 0, and solving).

Suppose now the ESPVR relation is nonlinear, but can be approximated by the parabolic expression (8,16):

$$P_{es} = a(V_{es} - V_o)^2 + b(V_{es} - V_o) \ . \tag{7}$$

Rewriting as

$$P_{es} = a(V_{ed} - V_o - SV)^2 + b(V_{ed} - V_o - SV) = Ea \cdot SV \tag{8}$$

substituting $V' = (V_{ed} - V_o)$ and rearranging, we get

$$a \cdot SV^2 - (Ea + b + 2V'a) \cdot SV + (aV'^2 + bV') = 0 \quad (9)$$

This quadratic equation can be solved for SV enabling prediction of stroke work, ejection fraction, etc. It can be easily shown that maximal work will still occur at the point at which the local ESPVR slope is equal to Ea. This applies to the parabolic fit used above, and in fact for any arbitrary monotonically increasing function $P_{es} = f(V_{es})$, (Appendix A). It should be noted that while the ESPVR may be nonlinear when determined over a very broad loading range, data obtained *in vivo* spanning physiologic operating ranges is often linear (20,28). Thus, for purposes of coupling analysis over similar load ranges before and after interventions, a linear model is often reasonable. However, coupling predictions should be viewed more cautiously when they are extrapolated beyond measured overlapping data.

II. Vascular Properties

> "Only in the case of young children do we find that the elasticity of the arteries is so perfectly adapted to the requirement of the organism as it is in the case of the lower animals."
>
> C.S. Roy, 1880 (44)

Since measurements of vascular impedance accurately describe the properties of the vasculature distal to the point of measurement, calculation of ascending aortic input impedance is accepted as being the most complete description of the hydraulic load faced by the left ventricle (33,41). The advantage of impedance as a descriptor of hydraulic load is that it characterizes the properties of the vascular bed independently of the cardiac input (2,41,54). Despite its many advantages, however, it is difficult to use impedance in models of coupling since it is a complex quantity and, hence, not expressed as a single real number whose value may increase or decrease with various interventions. In addition, indices of ventricular function are most often expressed in the time domain making it difficult to interface with vascular parameters in the frequency domain. While some workers have attempted to model ventricular function in the frequency domain (11), the most fruitful approach to studying coupling has been to approximate impedance measures of the vasculature by a three-element Windkessel model. This latter model has been further simplified to deal solely with total resistance (peripheral resistance and characteristic impedance) (50).

There are several levels of assumptions made in the use of these simpler models to describe vascular properties. Studies of coupling assume that the vascular parameters, like the ventricular properties, are linear and are independent of changes in cardiac parameters. This will be addressed further below. The important feature of any Windkessel model is that its properties are lumped into discrete variables since it is assumed that all events occur in the elastic chamber simultaneously. Such a model cannot incorporate a finite velocity of wave propagation or the effects of wave reflection. The utility of such a model of the systemic vasculature in studies of coupling was tested by Burkhoff *et al.* (5). They showed that in dogs the three-element Windkessel model predicts stroke volume, stroke work, oxygen consumption, and systolic and diastolic aortic pressures reasonably close to those found with a true impedance when model

or actual impedance were loaded onto a computer simulated left ventricle. However, the Windkessel model could not accurately predict aortic pressure and flow waveforms since these were largely determined by the timing of wave reflections. Nevertheless, in this study, a Windkessel load embodied sufficient information to predict many of the typical variables used in coupling studies.

There are several important limitations. Firstly, the impedance data were obtained in anesthetized, open-chest, reflex-blocked dogs in which vascular distensibility was high and wave reflections minimal. This makes the applicability to human studies less clear. In human subjects impedance patterns differ from such experimental animals (35,40), due to the increased stiffness of the adult human vasculature compared to adult canine vessels and to increased effects of wave reflections. Such differences have been shown in applications of a T-tube model of the systemic circulation to canine (38,41) versus human (40) aortic impedance data. The higher frequencies of impedance minima found in human aortic impedance plots have been related to asymptomatic arterial degeneration particularly in the descending aorta (4). Similarly, the ascending aortic pressure wave contour in human adult subjects shows a late systolic peak which is not found in canine studies. This pressure wave contour has been shown to be due to effects of wave reflection (35). Finally, as discussed by Burkhoff *et al.* (5), the aortic input impedance pattern and amount of wave reflection is known to be modified not only by the normal aging process (35) but also in disease states such as hypertension (55) and congestive heart failure (24). It may therefore be unwise to extrapolate results of comparisons between true impedance and Windkessel afterloads in the canine model to ventriculo-vascular coupling in adult humans or pathophysiological states.

The further reduction of the 3-element Windkessel model to a pure resistance load is made when coupling is modeled in terms of mean pressure and flow. These approximations assume that the pulsatile component of arterial load is small compared with peripheral resistance. Such assumptions may be valid for normal canine ventriculo-arterial coupling but pulsatile load becomes a significant part (up to 50%) of the total external ventricular load when the aortic impedance indicates significant effects of arterial stiffening and wave reflection (35).

As mentioned above, more complex modeling of ventriculo-arterial interaction has loaded impedance data directly onto models of ventricular function using the impulse response as a time-based equivalent representation of arterial impedance (5,26). Although such an approach circumvents the assumptions made using lumped models of the circulation and takes into account the effects of wave reflections, it still assumes that vascular impedance is linear (that is not dependent on mean pressure or flow) and not effected by cardiac performance. Such assumptions have been tested theoretically and in animal studies (1,27,28,37,41,54). Aortic impedance has been shown to be clearly independent of heart rate (5,37,54). Several studies have shown independence of impedance from alterations in ventricular flow waves induced pharmacologically or by efferent vagal stimulation (1,27,41), and from effects of changes in primary mean arterial pressure (2). In this latter study performed in anesthetized open-chest reflex-blocked dogs, Alexander *et al.* showed that Windkessel parameters of impedance were not altered by changes in mean arterial pressure over a range of 120 mmHg. However, indices of wave reflection were altered by mean pressure as a consequence of changes in pulse wave velocity. Again, whether these results are applicable to human impedance data is unknown, as the stiffer vasculature in human subjects may

exhibit more load-dependent nonlinearities than found with the compliant animal vasculature. In Latham's study of hypertensive baboons (25), the variation in coupling data may have been due to such nonlinearities.

Despite potential limitations in the assumptions used, the simplicity of the 3-element Windkessel model has facilitated many coupling studies. In particular, the use of *Ea* as a vascular parameter has great applicability in interfacing with the time-varying elastance model of ventricular function. Studies in the isolated canine hearts have confirmed the equivalence between *Ea* derived from the ventricular P_{es}/SV ratio and *Ea* derived from Windkessel parameters of impedance (Eq. 1). In open-chest, autonomically blocked dogs the approximation of P_{es}/SV by impedance parameters is excellent: $P_{es}/SV = 1.05Ea + 0.26$ ($r^2 = 0.988$) (Fig. 3). Somewhat analogously to the mean pressure influence on impedance spectra, we have tested whether *Ea* is altered by changes in systolic pressure. Loading was varied in six open chest dogs by left atrial hemorrhage, with pressure-volume data determined by the conductance catheter technique (20,21). Ea was determined for each beat by the P_{es}/SV ratio where P_{es} was defined as the point of maximal elastance $[P/(V - V_o)]$ for each P-V loop. The data were obtained before and after sympathetic blockade by i.v. propranolol, and normalized such that each run started at high preload with $Ea = P_{es} = 1.0$. The results (Fig. 4) showed that, with intact reflexes, Ea was little changed with as much as 20% reduction in P_{es} (via lowered preload), however, additional P_{es} reduction resulted in as much as a 100% increase in *Ea*. With reflex blockade, *Ea* was virtually constant despite nearly 50–60% reductions in end-systolic pressure.

But what of the applicability of the *Ea* concept to studies of coupling in adult humans or those with hypertension? Experience from previous studies of impedance and pressure waveforms (see above) would seem to indicate that the effects of vascular stiffening and increased wave reflection would invalidate the underlying assumptions

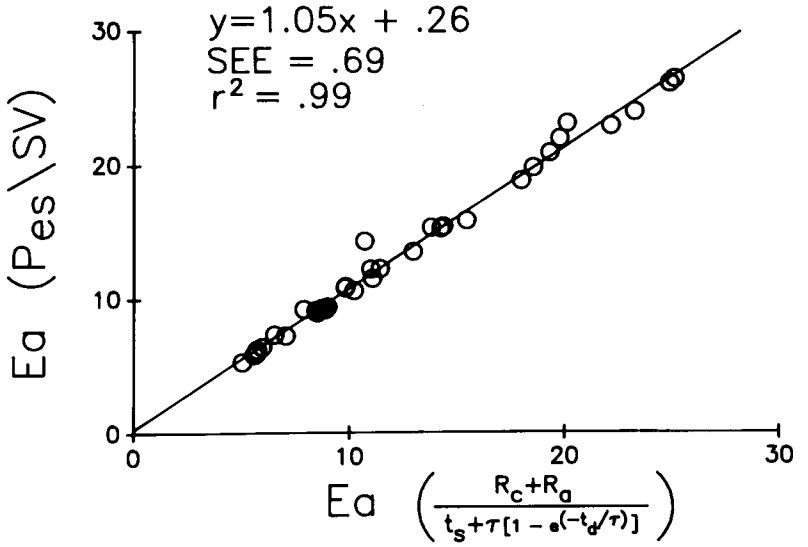

FIGURE 3. Comparison of *Ea* estimated from the ratio of P_{es}/SV versus that obtained from the impedance parameters using Eq. 1. See text for details. The two estimates correlated very well with a slope near 1.0.

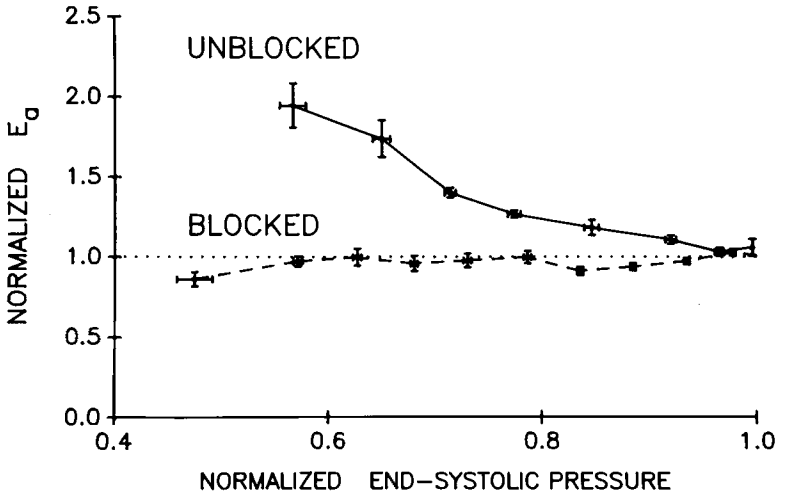

FIGURE 4. Influence of altered filling volume and thus end-systolic pressures on *Ea* estimates in anesthetized dogs. Baseline values for *Ea* and P_{es} were normalized to 1.0, and average data from six animals are shown. Prior to β-blockade, reduction of preload lowered P_{es} by 40–50% and led to nearly a doubling of *Ea*. After blockade, however, there was essentially no change in *Ea* over a broad range of operating pressures.

in the use of Ea. We recently addressed this issue in a study of eight human subjects at cardiac catheterization (22). Ea comparisons were made using the same two estimates (ventricular P_{es}/SV ratio, and ratio obtained from 3-element Windkessel impedance parameters [Eq. 1]) as displayed in Fig. 3. Aortic impedance was measured by micromanometer-flow catheter with simultaneous pressure-volume loops obtained by conductance catheter in eight human subjects aged 19 to 60 years. The patient group included both normal and aged, hypertensive vasculatures. In the older, hypertensive subjects, the loop contour displayed a characteristic rise during ejection to a late systolic peak. With rapid preload reduction (by IVC occlusion), the loops no longer manifested this late peak (Fig. 5), consistent with changes in the magnitude and/or timing of wave reflections and load dependence of arterial compliance. *Ea* estimates were compared before and after such loading change, as well as with pharmacologic intervention (captopril and verapamil). Despite evidence of arterial stiffening and wave reflections in these subjects, the two *Ea* estimates agreed very well: $P_{es}/SV = 0.98Ea + 0.1$ ($r^2 = 0.98$, $p < .0001$), falling along the identity line. Thus, both canine studies and preliminary results in normal and hypertensive human studies suggest that despite the approximations, *Ea* remains a useful description of arterial load *in vivo* for coupling studies.

PREDICTING INTEGRATED CARDIOVASCULAR FUNCTION

"The value of a principle is the number of things it will explain"

Emerson

A principal focus of ventriculo-vascular coupling analysis, and certainly one with direct clinical applicability, is the ability to predict integrated cardiovascular perfor-

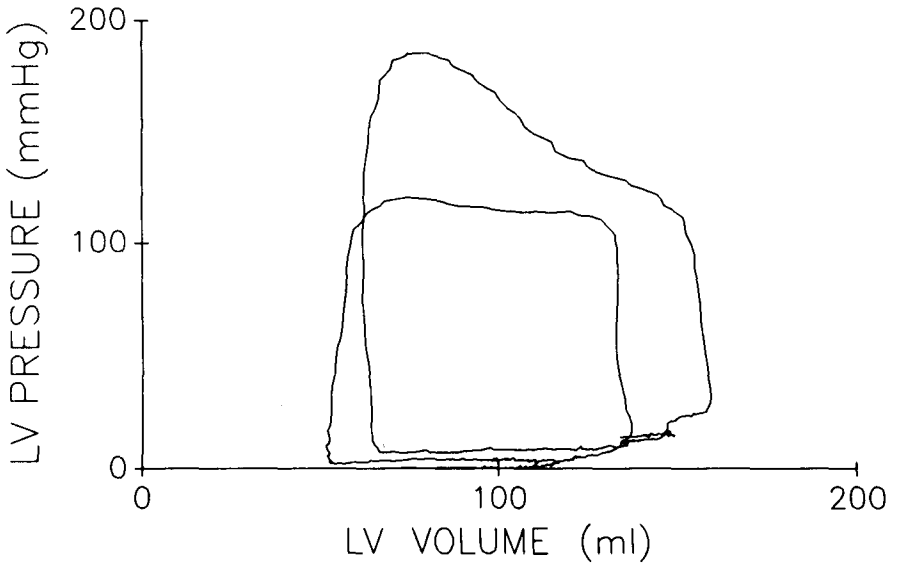

FIGURE 5. Influence of load range on pressure-volume loop shape in a hypertensive human subject. At normal preload, the loop displays systolic pressure rise with a late peak at end-systole. This contour can be rapidly changed by preload reduction (IVC occlusion) to a square loop. Since loop shape correlates with vascular impedance loads, this suggests that impedance spectra also vary as a function of volume load in such patients, complicating coupling analysis.

mance based on separate changes in either ventricular or vascular properties. Frameworks matching ventricular-to-arterial elastances or resistances describe mean behaviors, and thus can only predict integrated variables such as stroke volume, stroke work, ejection fraction, or mean pressure and flow. To more precisely predict ventricular and vascular pressure/flow waveforms, a complex impulse response derived from impedance spectra is required. However, even the ability to predict mean parameter change from pharmacologic interventions, for example, would be of great practical value. Again, we will focus the discussion on pressure-volume analysis, however, it is noted that anlogous data has been presented using mean pressure-flow relations.

In isolated hearts "ejecting" into a simulated 3-element Windkessel arterial system, it is easy to test the model framework expressed in Eqs. 3–6 above. This was first done by Sunagawa *et al.* (50), using Eq. 5 to predict stroke volume, and then comparing this value to measured stroke volume under a variety of loading conditions. Predicted and observed data agreed very well. The model was also successful in predicting stroke work by Eq. 6. Comparisons between predicted and measured stroke work in isolated hearts have also shown remarkable agreement (Fig. 6). Similar favorable comparisions have been obtained for *in situ* hearts ($SW_{measured} = 0.9 \cdot SW_{predicted} + 128$ mmHg·ml, $r = .85$, $n = 256$, $p < .001$).

In another study, Kass *et al.* (19) experimentally determined the loading and inotropic sensitivity of multiple indices of chamber systolic function. Experimental data for parameters such as ejection fraction, dP/dt_{max} and maximal velocity of circumferential shortening were obtained from pressure-volume data in isolated ejecting ca-

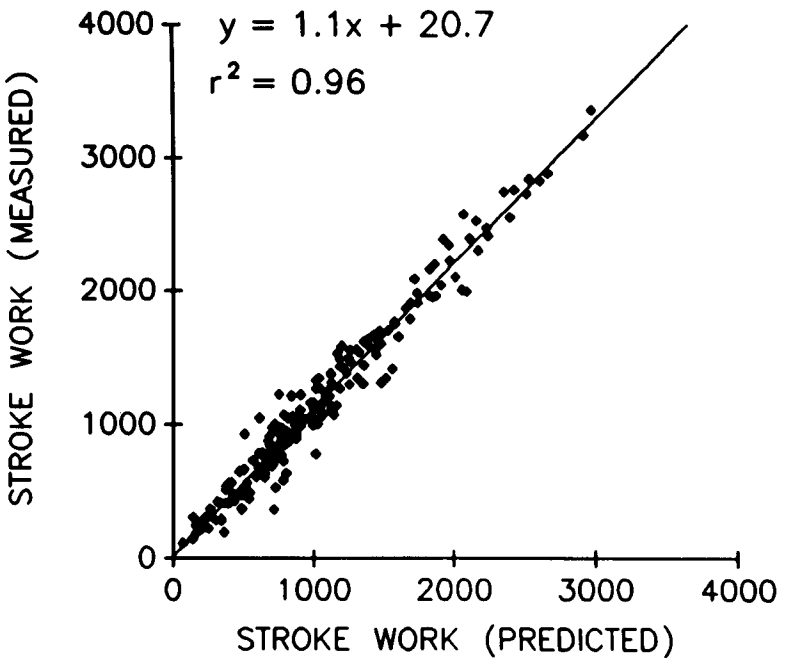

FIGURE 6. Predicted stroke work (using Eq. 6 modified to include assessment of area under the diastolic pressure-volume relation) and measured SW in isolated canine hearts. Comparisons were made over a wide range of contractile states and afterloads (*Ees* from 2.1 to 31.8, and *Ea* from 2.6 to 11.0 mmHg/ml), and the two values correlated very well.

nine left ventricles. The results were compared to predicted responses based on a theoretical analysis of the preload, afterload, and inotropic sensitivities of each index derived by pressure-volume coupling analysis. Both the experimental data and theoretical predictions compared very well for all indices studied. In addition to demonstrating the interrelationships between many systolic performance variables, these results further confirmed the usefulness of the pressure-volume coupling approach.

We have recently employed this framework to assess vascular versus ventricular effects of the pharmacologic agent amrinone in the intact dog (17). Since this drug has both vasodilator and positive inotropic effects, integrated responses (in flow or ejection fraction) are difficult to interpret in intact animals and man. By characterizing contractile state change by *Ees*, and arterial resistance change by *Ea* (heart rate was fixed and animals were autonomically blocked), both effects were easily separated and quantified. We assumed that each variable primarily reflected changes in its respective system, but accepting this premise, the drug clearly was shown to have marked effects on both. In a further (and first *in vivo*) test of the coupling approach, we used Eq. 5 (for stroke volume) divided by EDV to predict ejection fraction. The starting values of *Ees*, *Ea*, V_o, and EDV were entered into the equation, and then percent changes in *Ees* and *Ea*, observed after drug administration, were used to predict net EF changes for comparison to the actually measured EF changes. The coupling framework also enabled estimation of the separate contributions to the net EF change due to cardiac versus vascular changes. The results (Fig. 7) showed excellent agree-

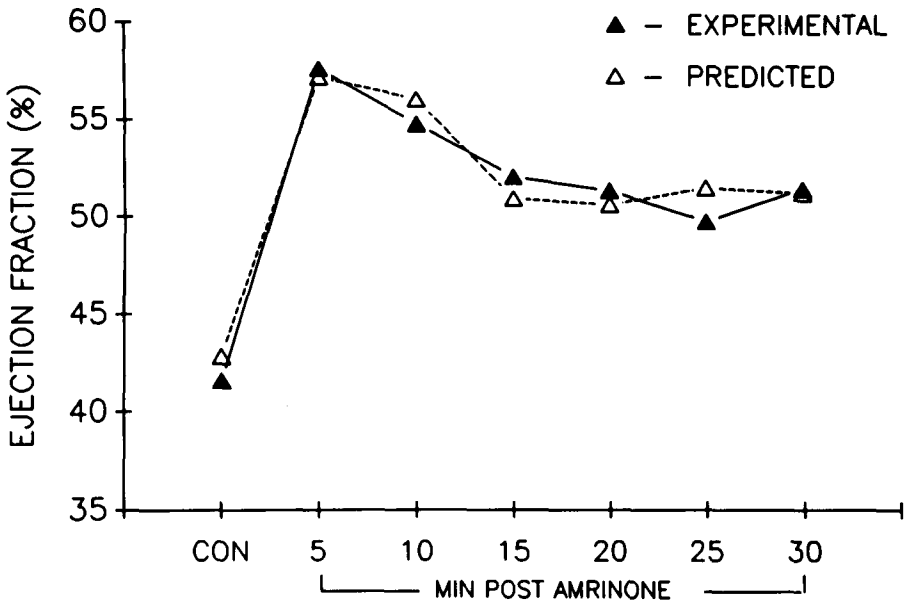

FIGURE 7. Comparison of predicted versus measured ejection fraction from seven closed-chest anesthetized dogs before and after i.v. amrinone bolus. Combined afterload reduction and contractile enhancement resulted in the net *EF* change, and the coupling model was used to predict the net change as a result of measured percent changes in *Ees* and *Ea* respectively. The result compared closely with the measured *EF* data (see [17]).

ment between experimental and predicted EF response. To date, these data represent the most direct evidence that the ventriculo-vascular coupling model can be used to take data obtained *in vivo* under one set of operating conditions, and use it to predict the response under an entirely new set of conditions.

OPTIMIZATION

Given a characterization of ventricular and vascular properties in terms that are easily coupled and which can accurately predict integrated pump performance, the next question regards how these variables actually couple *in vivo*. Theoretically, ventriculo-vascular interaction could be such that maximal work or power is generated, maximal myocardial efficiency (work/oxygen consumption) achieved, or neither.

Two studies published at almost the same time examined this issue from two different model perspectives. In a systematic analysis of isolated hearts, Sunagawa *et al.* (51) varied the arterial resistance (R) over a wide range under a variety of steady state conditions to determine the R value at which stroke work (SW) was maximal. Changes in inotropic state which increased the slope of the ESPVR also increased the R value at maximal SW, whereas changes in EDV did not. Increasing compliance (of the computer simulated 3-element Windkessel circuit) also led to a small but significant increase in arterial resistance at optimal SW. These results were very consistent with the ventriculo-arterial elastance coupling model outlined above in Eqs. 1 and 3-6. The prediction was that optimal stroke work would occur when $Ees = Ea$. Since, for

example, changes in EDV did not alter either ventricular or arterial elastance values (in the isolated heart preparation), the resistance at optimal coupling was not changed. On the other hand, since *Ees* increased with inotropic stimulation, *Ea* (and *R*) increased at optimal SW.

The prediction of matched elastances also leads to prediction of an ejection fraction (EF) of $\approx 50\%$. Since from Eq. 3

$$EF = \frac{SV}{V_{ed}} = \frac{Ees(V_{ed} - V_o)/(Ees + Ea)}{V_{ed}} \tag{10}$$

and if V_o is small (i.e., near 0) and $Ees = Ea$, then

$$EF = \frac{Ees(V_{ed} - 0)/(Ees + Ees)}{V_{ed}} = \frac{1}{2} \,. \tag{11}$$

While it is recognized that normal intact human subjects have EF values generally greater than 50%, this value is typical of anesthetized animals. Thus, it is perhaps less surprising that in the *in situ* heart study of open chest cats (58), that appeared at about the same time as the above mentioned isolated heart study, the equilibrium coupling point was indeed similar. The framework used in this latter study involved mean ventricular pressure-flow relations and matched ventricular source resistance to arterial resistance to predict mean power. Under baseline conditions, matching was found near optimal power (equivalent to optimal SW at a given heart rate). As in the isolated heart study, increasing heart rate did not significantly alter the working point. However, in neither study were heart rate changes physiologic (120–160 in the isolated heart, and 180–200 min^{-1} for the cat study). Heart rate effects on coupling in normal physiologic ranges may be greater.

While altering volumes or heart rate did not appear to move the coupling point away from that predicted for optimal power (or work), acute inotropic changes had a different effect. In one study, norepinephrine markedly increased the coupling work point (R_p/R_s, analogous to *Ea/Ees*), moving it away from optimal power (56). Myhre *et al.* (36) similarly showed that depression of ventricular function also shifted the coupling set point away from optimal work. Thus, if in fact normal resting physiologic controls are such that the operating coupling point is at or near maximal power (or stroke work), these data indicated that such coupling is not tightly controlled by some "optimizing" feedback circuit, but could be acutely over-ruled by various interventions. However, these drugs could represent extreme and unbalanced interventions (i.e., heart vs. vasculature). Under more normal physiologic conditions, such as exercise, optimal coupling appears preserved (49).

These series of studies and observations raise several questions. First, since matching of *Ea* and *Ees* (or R_p and R_s) predicts an ejection fraction near 50%, and intact human (and animal) EFs are generally higher (60–70%), is it possible that something other than power or work is optimized in intact systems? This issue was raised and theoretically examined by Burkhoff and Sagawa (7). Using a linear ESPVR, *Ea*, and the linear relation between oxygen consumption (MVO_2) and pressure-volume area (PVA), these authors generated equations to predict coupling ratios at optimal work as well as optimal efficiency (SW/MVO_2) (Appendix B). Using "typical" left heart data (*Ees* = 7 mmHg/ml, V_o 5 ml, EDV = 35 ml) and normal values for slope and

intercept of an MVO_2-PVA relation ($2.4 \cdot 10^{-5}$ mlO_2/beat/mmHg·ml, and 0.04 mlO_2/beat respectively) the model predicted optimal work at an *Ees/Ea* ratio of 1.0, but optimal efficiency at a ratio of 2.0. With a ratio of 2.0, EF is predicted to be between 60–70%, consistent with human data, and thus the authors suggested that efficiency rather than work or power may be optimized in intact systems.

There are a few problems with the analysis, however. The equation for efficiency derived by Burkhoff is a function of *Ees*, *Ea*, V_{ed}, and V_o. Using this expression, one can obtain an analytic solution for the *Ees/Ea* ratio at maximal efficiency (Appendix B). However, rather than being a constant at *Ees/Ea* = 2.0, the result is nonlinear and itself a function of both *Ees* and V_{ed} (Fig. 8). The value of 2.0 results from the particular (albeit representative for normal heart) numbers used in the modeling study (7), but could vary depending on preload or myocardial function. Thus, while it is intriguing that recent values for this coupling ratio in both conscious animals and humans have been reported near 1.5 (3,59) or more, it is less clear whether this actually represents efficiency optimization.

Ultimately, determining what is optimized by studying the numeric ratio of coupling parameters is unlikely to be very fruitful. In experimental studies of work and efficiency optimization, and indeed as predicted from theoretical analyses of these relations (7,51), "optimum" coupling points fall on curves that are rather shallow over a broad range. Thus, coupling ratios can be varied over a wide range while still remaining at 95% or more of both maximal work and efficiency (15).

One interesting side issue is how nonlinear ESPVRs might effect the peaked nature of optimization curves. Figure 9 shows results of a theoretical analysis for both SW and efficiency as functions of coupling ratio for linear and nonlinear cases. Each

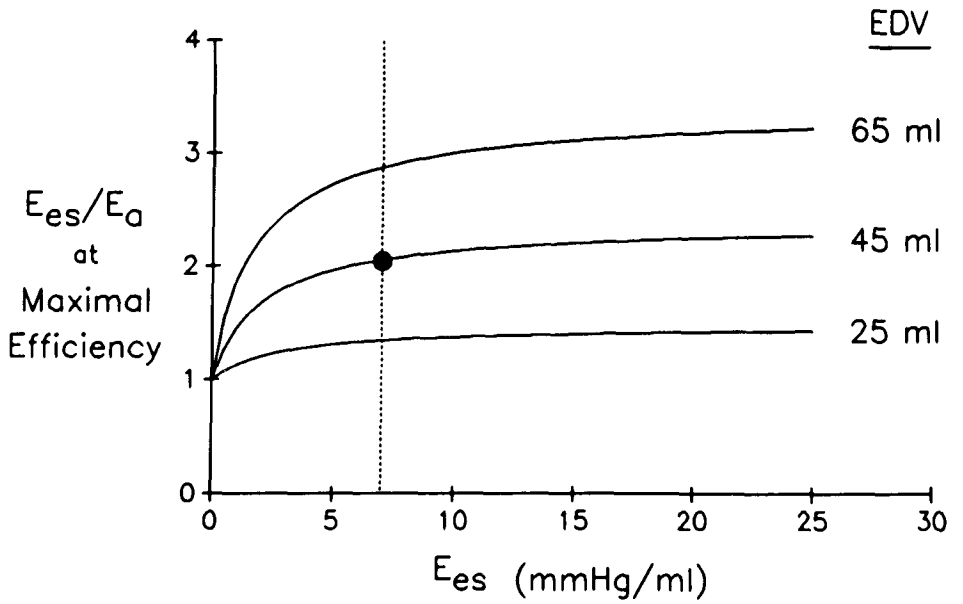

FIGURE 8. Theoretical model result showing the influence of *Ees* and V_{ed} on the *Ees/Ea* coupling ratio at optimal efficiency. Rather than always being 2.0, this ratio varies as a function of both *Ees* and V_{ed}. At the parameter values used by Burkhoff (7), this results in a ratio of 2.0. However, for larger or depressed hearts, the ratio could be different and still be at optimal efficiency.

variable is normalized to a value of 1.0 at maximum. Curves lying above the dotted line (95%) are within 5% of optimal work or efficiency respectively. For stroke work, ESPVR nonlinearity has the effect of broadening out the optimal range to almost double that for the linear model. This *in vivo* nonlinearity would be expected to make optimal (or near optimal) work obtainable over an even broader range of coupling ratios. As noted previously, and shown in Appendix A, optimal work is achieved at the identical coupling ratio for both linear and nonlinear ESPVRs. Efficiency is less affected by a nonlinear ESPVR, and although the optimal point is shifted slightly, there is little physiologic impact as both relations are quite flat.

Another more intriguing issue centers on what controls coupling *in vivo*. Is the ob-

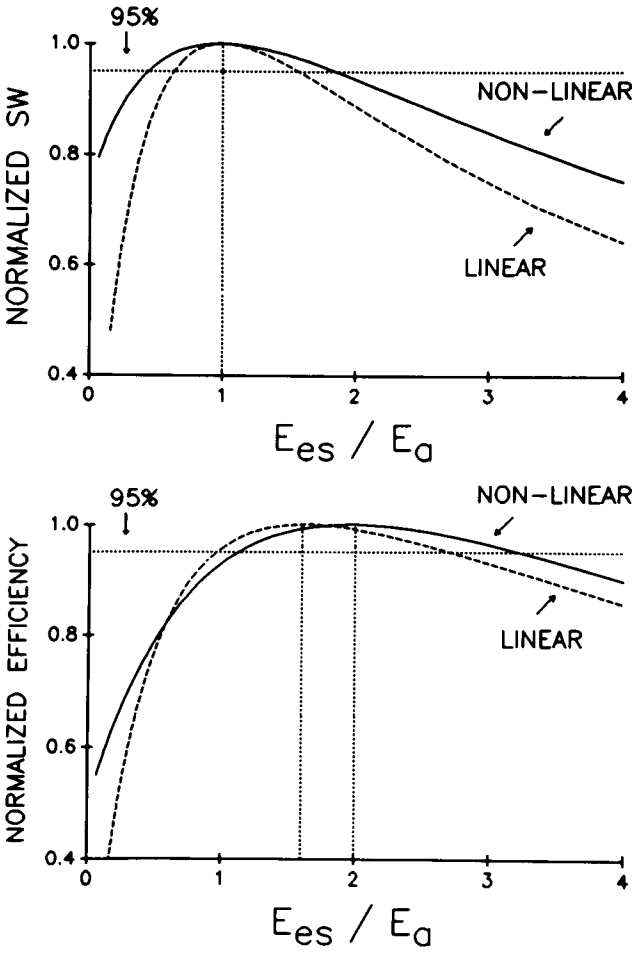

FIGURE 9. Theoretical model result of effect of ESPVR nonlinearity on stroke work and efficiency versus coupling ratio relations. For stroke work (Top) nonlinear ESPVR would be expected to flatten out this relation further, substantially extending the range of coupling ratios at which work (or power) is at 95% or more of maximal. The optimal point is at *Ees* = *Ea* for linear and nonlinear case as predicted (Appendix A). For efficiency relations (lower panel), the two curves are more similar both peaking at coupling ratios >1.0. More importantly, the range of coupling ratios at or above 95% efficiency is very broad and overlaps the optimal work ratio of 1.0.

servation that coupling *in vivo* is near optimal power (or efficiency) serendipitous, or is a control system involved? Recent reports on conscious animals undergoing treadmill exercise indicate that ventriculo-arterial coupling is matched at near maximal work (or power) and remains matched throughout exercise (49). This seems remarkable since it implies that during a complex event such as exercise in which heart rate, fluid shifts, contractility, and vascular properties are *all* altered, optimal coupling for maximal work is maintained. As noted by Van den Horn *et al.* (56), it is unlikely that there are power (or work) receptors, certainly none have been described, nor are efficiency receptors known to exist. Looking to well characterized mechanoreceptors, both cardiac stretch receptors and vascular baroreceptors are potential controllers. In a recent intriguing study (23), random noise pressure perturbations were imposed on an isolated carotid sinus in anesthetized dogs, and the transfer function between coronary sinus pressure (CSP) and ventricular and arterial elastances determined. The results showed that a step response of CSP produced an instantaneous ratio of *Ea/Ees* of 0.93 ± 0.21, not significantly different from 1.0, thus maintaining optimal work or power. It would appear that feedback control on both heart and vasculature during normal exercise may well maintain coupling at near optimal ratios.

The third and last question, which is only beginning to be explored, is whether coupling and/or coupling control mechanisms are altered in disease states. In a baboon study, Latham *et al.* (25) found that chronic hypertension (increased *Ea*) induced by perinephritis led to ventricular hypertrophy and increases in end-systolic elastance. However, the coupling between these parameters was complex, and highlighted a problem facing investigators of disease conditions: that characterization of coupling and the assessment of vascular properties often varies with the mean level of systolic arterial pressure. While vascular properties are more constant over physiologic operating ranges in normal vasculatures, hypertension increases late systolic wave reflections and pushes the operating point to a less compliant range. From this baseline, increases or decreases in mean arterial pressure or volume are more likely to alter the compliance or magnitude of reflections (see Fig. 5) making impedance (and *Ea*) dependent on ventricular properties (i.e., pressures or stroke volume), and coupling analysis more difficult.

In another recent study, Asanoi *et al.* (3) reported on coupling ratios in normal human subjects and in subjects with ventricular dysfunction. They found *Ees/Ea* was approximately 2.0 for normals (EF 66%), 1.0 for patients with mild cardiac depression (EF 50%), and 0.5 in heart failure patients (EF 29%). The authors suggested that normal coupling may work at optimal efficiency, whereas in mild heart failure, optimal work is achieved. However, our analysis above suggests this differentiation may not be very meaningful. One can conclude that with clinical myocardial depression (as true of animal data [36]), coupling is no longer maintained at optimal work (or efficiency), but responds to demands for adequate peripheral perfusion pressure. Given data that have shown abnormalities of baroreflex control during exercise in heart failure patients (9,34), it is interesting to speculate that coupling ratios might deteriorate further under stress. Increasing impedance mismatch with exercise could be one source of integrated cardiovascular compromise in patients with such diseases. This question is as yet unexplored.

SUMMARY

As a tool for understanding integrated cardiovascular performance, studies of ventriculo-vascular coupling have already proven to be very valuable. As an approach

for predicting system performance under an entirely new set of operating conditions, data from isolated or autonomically blocked hearts show excellent agreement between measured and predicted responses. However, data from intact animals with normal closed-loop physiological feedback controls present a far more complex test, and more study is needed. Examination of a variety of questions regarding coupling in humans is only beginning but looks to be promising. Given the development of fast computers and thus greater ease of coupling more comprehensive descriptions of vascular properties in the frequency domain with ventricular properties in the time domain, we may look to studies on the interaction between physiologically relevant vascular loading abnormalities and ventricular performance. Improvements in understanding the interactions between vascular load and ventricular function will undoubtedly lead to greater insights and ability to predict responses in intact systems. We expect that by the time another review on this topic appears in this journal, many of the complexities affecting both ventricular and vascular characterization, and the influences of intact control systems on these parameters and their coupling, will be better understood.

REFERENCES

1. Abel, F.L. Fourier analysis of left ventricular performance. Circ. Res. 28:119–135; 1971.
2. Alexander, J.; Burkhoff, D.; Schipke, J.; Sagawa, K. Influence of mean pressure on aortic impedance and reflections in the systemic arterial system. Am. J. Physiol. 257:H969–H978; 1989.
3. Asanoi, H.; Sasayama, S.; Kameyama, T. Ventriculo-arterial coupling in normal and failing heart in humans. Circ. Res. 65:483–493; 1989.
4. Avolio, A.P.; Chen, S.G.; Wang, R.P.; Zhang, C.L.; Li, M.F.; O'Rourke, M.F. Effects of age on changing arterial compliance and left ventricular load in a northern Chinese urban community. Circulation 68:50–58; 1983.
5. Burkhoff, D.; Alexander, J.; Schipke, J. Assessment of Windkessel as a model of aortic input impedance. Am. J. Physiol. 255:H742–H753; 1988.
6. Burkhoff, D.; de Tombe, P.P.; Hunter, W.C.; Kass, D.A. Contractile strength and mechanical efficiency of left ventricle are enhanced by physiologic afterload. Am. J. Physiol. 260 (Heart Circ. Physiol. 29):H569–H578; 1991.
7. Burkhoff, D.; Sagawa, K. Ventricular efficiency predicted by an analytical model. Am. J. Physiol. 250 (Regulatory Integrated Comp. Physiol.): R1021–1027; 1986.
8. Burkhoff, D.; Sugiura, S.; Yue, H.; Sagawa, K. Contractility-dependent curvilinearity of end-systolic pressure-volume relations. Am. J. Physiol. 252 (Heart Circ Physiol 21): H1218–H1227; 1987.
9. Cohn, J.N. Abnormalities of peripheral sympathetic nervous system control in congestive heart failure (Review). Circulation 82:2 Suppl I59–67; 1990.
10. Elzinga, G.; Westerhof, N. The effect of an increase in inotropic state and end-diastolic volume on the pumping ability of the feline left heart. Circ. Res. 42:620–628; 1978.
11. Elzinga, G.; Westerhof, N. End-diastolic volume and source impedance of the heart. In: The physiological basis of Starling's Law of the heart. Ciba Foundation Symposium; 1974: 24:242–255.
12. Freeman, G.L.; Little, W.C.; O'Rourke, R.A. The effect of vasoactive agents on the left ventricular end-systolic pressure-volume relation in closed-chest dogs. Circulation 74:1107–1113; 1986.
13. Hunter, W.C. End-systolic pressure as a balance between opposing effects of ejection. Circ. Res. 64:265–275; 1989.
14. Hunter, W.C.; Alexander, J.; Ifarraguerri, A. Effect of arterial wave reflections on the coupling between left ventricle and aorta. Proceedings of the 9th International Conference of the Cardiovascular System Dynamics Society, Halifax, N.S., Canada. 1988: pp. 177–180.
15. Jones, S.R.; de Tombe, P.P.; Burkhoff, D.; Kass, D.A. Optimization of total ventricular efficiency studied in isolated canine hearts (Abstract). Circulation 82:III-695; 1990.
16. Kass, D.A.; Beyar, R.; Lankford, E.; Heard, M.; Maughan, W.L.; Sagawa, K. Influence of contractile state on curvilinearity of *in situ* end-systolic pressure-volume relations. Circulation 79:167–178; 1989.
17. Kass, D.A.; Grayson, R.; Marino, P. Pressure-volume analysis as a method for quantifying simultaneous drug (amrinone) effects on arterial load and contractile state *in vivo*. J. Am. Coll. Cardiol. 16:726–732; 1990.

18. Kass, D.A.; Maughan, W.L. From 'Emax' to pressure-volume relations: A broader view. Circulation 77:1203–1212; 1988.
19. Kass, D.A.; Maughan, W.L.; Guo, Z.M.; Kono, A.; Sunagawa, K.; Sagawa, K. Comparative influence of load versus inotropic states on indexes of ventricular contractility: Experimental and theoretical analysis based on pressure-volume relationship. Circulation 76:1422–1436; 1987.
20. Kass, D.A.; Midei, M.; Graves, W.; Maughan, W.L. Use of a conductance (volume) catheter and transient inferior vena caval occlusion for rapid determination of pressure-volume relationships in man. Cath. Cardiovasc. Diag. 15:192–202; 1988.
21. Kass, D.A.; Yamazacki, T.; Burkhoff, D.; Maughan, W.L.; Sagawa, K. Determination of left ventricular end systolic pressure-volume relationships *in situ* by the conductance (volume) catheter technique in anesthetized dogs. Circulation 73:586–595; 1986.
22. Kelly, R.P.; Ting, C.T.; Maughan, W.L.; Chang, M.S.; Kass, D.A. Similarity of arterial elastance estimates from ventricular and vascular parameters in man (Abstract). Circulation 82:III-696; 1990.
23. Kobota, T.; Alexander, J.; Itaya, R.; Todaka, K.; Sugimachi, M.; Sunagawa, K. Dynamic matching of the left ventricle with the arterial system by carotid sinus baroreflex (Abstract). Circulation 82:III-695; 1990.
24. Laskey, W.K.; Kussmaul, W.G. Arterial wave reflection in cardiac failure. Circulation 75:711–722; 1987.
25. Latham, R.D.; Rubal, B.J.; Sipkema, P.; Westerhof, N.; Virmani, R.; Robinowitz, M.; Walsh, R.A. Ventricular/vascular coupling and regional arterial dynamics in the chronically hypertensive baboon: Correlation with cardiovascular structural adaptation. Circ. Res. 63:798–811; 1988.
26. Latson, T.W.; Hunter, W.C.; Burkhoff, D.; Sagawa, K. Time sequential prediction of ventricular-vascular interactions. Am. J. Physiol. 251:H1341–H1353; 1986.
27. Latson, T.W.; Hunter, W.C.; Katoh, N.; Sagawa, K. Effect of nitroglycerin on aortic impedance, diameter, and pulse wave velocity. Circ. Res. 62:884–890; 1988.
28. Little, W.C.; Cheng, C.P.; Peterson, T.; Vinten-Johansen, J. Response of the left ventricular end-systolic pressure-volume relation in conscious dogs to a wide range of contractile states. Circulation 78:736–745; 1988.
29. Little, W.C.; Freeman, G.L. Description of LV pressure-volume relations by time-varying elastance and source resistance. Am. J. Physiol. 253:H83–H90; 1987.
30. Maughan, W.L.; Sunagawa, K.; Burkhoff, D.; Sagawa, K. Effect of arterial impedance changes on the end-systolic pressure-volume relation. Circ. Res. 54:595–610; 1984.
31. Maughan, W.L.; Sunagawa, K.; Sagawa, K. Effects of arterial input impedance on mean ventricular pressure-flow relation. Am. J. Physiol. 247 (Heart Circ. Physiol. 16): H978–H983; 1984.
32. McKay, R.G.; Aroesty, J.M.; Heller, G.V.; Royal, H.D.; Grossman, W. Assessment of the end-systolic pressure-volume relationship in human beings with the use of a time varying elastance model. Circulation 74:97–104; 1986.
33. Milnor, W.R. Arterial impedance as ventricular afterload. Circ. Res. 36:565–570; 1975.
34. Mohanty, P.K.; Arrowood, J.A.; Ellenbogen, K.A.; Thames, M.D. Neurohumoral and hemodynamic effects of lower body negative pressure in patients with congestive heart failure. Am. Heart J. 118:78–85; 1989.
35. Murgo, J.P.; Westerhof, N.; Giolma, J.P.; Altobelli, S.A. Aortic input impedance in normal man: Relationship to pressure wave shapes. Circulation 62:105–116; 1980.
36. Myhre, E.S.P.; Johansen, A.; Piene, H. Optimal matching between canine left ventricle and afterload. Am. J. Physiol. 254:H1051–H1058; 1988.
37. Nobel, M.I.M.; Gabe, I.T.; Trenchard, D.; Guz, A. Blood pressure and flow in the ascending aorta of conscious dogs. Cardiovasc. Res. 1:9–20; 1967.
38. O'Rourke, M.F. Pressure and flow waves in systemic arteries and the anatomical design of the arterial system. J. Appl. Physiol. 23:139–149; 1967.
39. O'Rourke, M.F. Steady and pulsatile energy losses in the systemic circulation under normal conditions and in simulated arterial disease. Cardiovasc. Res. 1:313–316; 1967.
40. O'Rourke, M.F., Avolio, A.P. Pulsatile flow and pressure in human systemic arteries: Studies in man and in a multi-branched model of the systemic arterial tree. Circ. Res. 44:363–372; 1980.
41. O'Rourke, M.F.; Taylor, M.G. Input impedance of the systemic circulation. Circ. Res. 20:365–380; 1967.
42. Piene, H. Impedance matching between ventricle and load. Ann. Biomed. Eng. 12:191–207; 1984.
43. Piene, H.; Myhre, E.S.P. Left ventricle-aortic coupling: Prediction of contraction pattern. Am. J. Physiol. 247:H531–H540; 1984.

44. Roy, C.S. The elastic properties of the arterial wall. J. Physiol. 3:125–159; 1880.
45. Sagawa, K.; Maughan, W.L.; Suga, H.; Sunagawa, K. Cardiac contraction and the pressure-volume relationship. New York: Oxford University Press; 1988.
46. Schroff, S.G.; Janicki, J.S.; Weber, K.T. Evidence and quantification of left ventricular resistance. Am. J. Physiol. 249 (Heart Circ. Physiol. 18): H353; 1983.
47. Sodums, M.T.; Badke, F.R.; Starling, M.R.; Little, W.C.; O'Rourke, R.A. Evaluation of left ventricular contractile performance utilizing end-systolic pressure-volume realtionships in conscious dogs. Circ. Res. 54:731–737; 1984.
48. Suga, H.; Hayashi, T.; Sirahata, M. Ventricular systolic pressure volume area as predictor of cardiac oxygen consumption. Am. J. Physiol. 240 (Heart Circ. Physiol. 9): H320; 1981.
49. Sugimachi, M.; Sunagawa, K.; Todaka, K.; Hayashida, K.; Noma, M.; Ando, H.; Egashira, S.; Tomoike, H.; Nakamura, M. Does the canine left ventricle operate at the optimal contractility and heart rate to minimize oxygen consumption during exercise and left ventricular dysfunction? Proceedings of the 9th International Conference of the Cardiovascular System Dynamics Society, Halifax, N.S., Canada. 1988: pp. 227–230.
50. Sunagawa, K.; Maughan, W.L.; Burkhoff, D.; Sagawa, K. Left ventricular interaction with arterial load studied in isolated canine ventricle. Am. J. Physiol. 245:H773–H780; 1983.
51. Sunagawa, K.; Maughan, W.L.; Sagawa, K. Optimal resistance for the maximal stroke work studied in isolated canine left ventricle. Circ. Res. 56:586–595; 1985.
52. Sunagawa, K.; Sagawa, K.; Maughan, W.L. Ventricular interaction with the loading system. Ann. Biomed. Eng. 12:163–189; 1984.
53. Sunagawa, K.; Sagawa, K.; Maughan, W.L. Ventricular interaction with the vascular system in terms of pressure-volume relationships. In Yin, F.C.P., ed. Ventricular/vascular coupling. New York: Springer-Verlag; 1987: pp. 210–239.
54. Taylor, M.G. Use of random excitation and spectral analysis in the study of frequency-dependent parameters of the cardiovascular system. Circ. Res. 18:585–595; 1966.
55. Ting, C.T.; Brin, K.P.; Lin, S.J.; Wang, S.P.; Chang, M.S.; Chiang, B.N.; Yin, F.C.P. Arterial hemodynamics in human hypertension. J. Clin. Invest. 78:1462–1471; 1986.
56. Van den Horn, G.J.; Westerhof, N.; Elzinga, G. Feline left ventricle does not always operate at optimum power output. Am. J. Physiol. 250:H961–H967; 1986.
57. Van den Horn, G.J.; Westerhof, N.; Elzinga, G. Interaction of heart and arterial system. Ann. Biomed. Eng. 12:151–162; 1984.
58. Van den Horn, G.J.; Westerhof, N.; Elzinga, G. Optimal power generation by the left ventricle. Circ. Res. 56:252–261; 1985.
59. Winnem, B.M.; Piene, H. Left ventricular end-systolic pressure volume relations in healthy young men. Eur. Heart J. 7:961–972; 1986.

APPENDIX A

For a nonlinear end-systolic pressure volume relation, it can be easily shown that maximal stroke work will be achieved when *Ea* (the arterial elastance line) has a slope equal and opposite to the instantaneous slope of the nonlinear ESPVR.

Let the ESPVR be defined by the relation

$$P_{es} = f(V_{es})$$

where f is a monotonically increasing function of V_{es}. Then the local slope of the ESPVR ($Ees_{V_{es}}$) at a given V_{es} is $f'(V_{es})$. The *Ea* is the ratio of P_{es}/SV as defined for the linear case. Then we have

$$Ea = \frac{P_{es}}{SV} = \frac{P_{es}}{V_{ed} - V_{es}} = \frac{f(V_{es})}{V_{ed} - V_{es}} \tag{A1}$$

and

$$SW \approx P_{es} \cdot SV = f(V_{es}) \cdot (V_{ed} - V_{es}) \ . \tag{A2}$$

For a given end-diastolic volume (V_{ed}), the V_{es} that maximizes SW is:

$$\frac{dSW}{dV_{es}} = f'(V_{es})(V_{ed} - V_{es}) - f(V_{es}) = 0 \tag{A3}$$

or

$$f'(V_{es}) = \frac{f(V_{es})}{V_{ed} - V_{es}} \ . \tag{A4}$$

Since, $f'(V_{es}) = Ees_{V_{es}}$; and $f(V_{es})/(V_{ed} - V_{es}) = Ea$, then Eq. A4 indicates that optimal SW occurs when $Ees_{V_{es}} = Ea$.

APPENDIX B

As presented by Burkhoff and Sagawa (7), an analytic expression for optimization of efficiency can be derived from Eqs. 2, 3, and 6, and the energetics relation:

$$MVO_2 = aPVA + b \tag{B1}$$

where a and b are constants. PVA is the pressure-volume area defined as the sum of stroke work and a potential energy approximately equal to

$$PVA = SW + PE = P_{es} \cdot SV + P_{es} \cdot (V_{es} - V_o)/2 \tag{B2}$$

and MVO_2 is myocardial oxygen consumption. Myocardial efficiency is defined by the ratio of stroke work to MVO_2. Adding stroke work (Eq. 6) to the equation for potential energy yields PVA (Eq. B2) which is substituted into Eq. B1 to predict MVO_2. Dividing SW by predicted MVO_2 yields the following expression for efficiency:

$$EFF = \left[a(1 + (Ea/2Ees)) + \frac{b(1 + (Ea/Ees)^2)}{Ea(V_{ed} - V_o)^2} \right]^{-1} \ . \tag{B3}$$

For a fixed Ees, Eq. B3 can be differentiated with respect to Ea and set equal to zero in order to solve for the value of Ea (and thus Ees/Ea ratio) which optimizes efficiency. The result is:

$$Ees/Ea \ @ \ EFF_{\max} = \sqrt{[a(V_{ed} - V_o)^2 Ees/2 + b]/b} \ . \tag{B4}$$

For typical canine data parameter values as used in the model study of Burkhoff and Sagawa (7), (Ees = 7.0 mmHg/ml, V_{ed} = 45 ml, V_o = 5 ml, b = .05 ml O_2/beat, $a = 2.6 \cdot 10^{-5}$ ml O_2/beat/mmHg·ml), Eq. B4 yields a coupling ratio of 2.0. However, clearly for larger volumes and different contractile states, the predicted ventriculo-vascular coupling point at optimal efficiency will vary, and might be greater or less than 2.0 (see Fig. 8).